

Settling velocity, effective density, and mass composition of suspended sediment in a coastal bottom boundary layer, Gulf of Lions, France

K.J. Curran^{a,*}, P.S. Hill^a, T.G. Milligan^b, O.A. Mikkelsen^c, B.A. Law^b,
X. Durrieu de Madron^d, F. Bourrin^d

^aDepartment of Oceanography, Dalhousie University, Halifax, NS, Canada B3H 4J1

^bFisheries and Oceans Canada, Bedford Institute of Oceanography, 1 Challenger Dr., PO Box 1006, Dartmouth, NS, Canada B2Y 4A2

^cSchool of Ocean Sciences, University of Wales at Bangor, Menai Bridge, Anglesey, Wales LL59 5AB, UK

^dCentre de Formation et de Recherche sur l'Environnement Marin (CEFREM), CNRS—Université de Perpignan, Perpignan cedex 66860, France

Received 26 July 2006; received in revised form 27 November 2006; accepted 8 January 2007

Available online 31 January 2007

Abstract

Particle size distribution and size-specific settling velocity are critical parameters for understanding the transport of fine sediment on continental margins. In this study, observed floc size versus settling velocity, volume distributions of particles 2 μm –1 cm in diameter, and calculated effective densities for all particle sizes provided estimates of the mass distribution in suspension, which is used to apportion mass among component particles, microflocs, and macroflocs. Measurements were made during relatively quiescent environmental conditions. Observations of size distributions based on mass demonstrate an increase in the component particle fraction through time. The increase in the percentage of component particles in suspension had implications on water column properties, as small changes in the component particle fraction affected water column optical transmission in a way that was not as easily detected by changes in the volume concentration distribution or total mass concentration. Flocs larger than 133 μm in diameter only comprised one quarter to one third of the mass in suspension. This finding may explain why suspension bulk clearance rates are often an order of magnitude lower than those predicted by other methods.

© 2007 Elsevier Ltd. All rights reserved.

Keywords: Fine sediment; Flocs; Settling velocity; Effective density; Particle size distribution; Mass composition; Gulf of Lions; France

1. Introduction

In marine environments, the transport and deposition of fine sediment depend on the abundance and size of flocs. Floc size and abundance are controlled by sediment concentration and turbulence, which affect the suspended particle size distribution. The settling flux of fine sediment to

*Corresponding author. Tel.: 1 902 494 6717;

fax: 1 902 494 3877.

E-mail addresses: kcurran@dal.ca (K.J. Curran),
phill@phys.ocean.dal.ca (P.S. Hill),
milligant@mar.dfo-mpo.gc.ca (T.G. Milligan),
oss202@bangor.ac.uk (O.A. Mikkelsen),
lawb@mar.dfo-mpo.gc.ca (B.A. Law), demadron@univ-perp.fr
(X. Durrieu de Madron), fbourrin@univ-perp.fr (F. Bourrin).

the seabed is dependent upon size-specific particle settling velocities and on the distribution of mass among different-sized particles in suspension. Studies that have estimated settling velocity of fine sediment particles in various marine environments (e.g. estuaries, fjords, and coastal environments) demonstrate that particles ranging from $1\ \mu\text{m}$ to several millimeters in diameter exhibit settling velocities ranging from 0.001 to $>10\ \text{mm s}^{-1}$, with the settling velocity generally increasing with increased particle size (Dyer et al., 1996; Hill et al., 1998; Dyer and Manning, 1999; Sternberg et al., 1999; Mikkelsen and Pejrup, 2001; Fox et al., 2004; Xia et al., 2004). From a size versus settling velocity relationship a size-specific effective density can be estimated by re-arranging Stokes' Law. Particles ranging from $1\ \mu\text{m}$ to several millimeters in diameter exhibit effective densities ranging from 1 to $>1000\ \text{kg m}^{-3}$, with the effective density generally decreasing with increased particle size (Hill et al., 1998; Dyer and Manning, 1999; Sternberg et al., 1999; Fox et al., 2004; Xia et al., 2004).

To estimate the settling flux of mass to the seabed, temporal observations of the in situ particle size distribution are required (Agrawal and Pottsmith, 2000). Eisma (1986) provided a simplified characterization of floc dynamics in suspension, where the in situ particle size distribution is partitioned into 'microflocs' and 'macroflocs'. Microflocs are small, tightly packed flocs approximately less than $125\ \mu\text{m}$ in diameter. They are composed of smaller grains bound by organic matter. Macroflocs are porous, loosely bound flocs approximately greater than $125\ \mu\text{m}$ in diameter. They are primarily composed of microflocs. Eisma (1986) argued that macroflocs are fragile and easily broken into their microfloc constituents, and that microflocs are more robust and not as easily broken into their constituents. For simplicity, a similar characterization of the suspended particle size distribution is employed in this study to apportion mass in suspension, whereby constituent particle sizes less than microflocs are termed 'component particles'.

Floc fraction, f , is defined as the fraction of mass in suspension bound within flocs. Various methods have been used to quantify f (Syvitski et al., 1995; Mikkelsen and Pejrup, 2001; Curran et al., 2002, 2004a; Fox et al., 2004). The Stokes' Law method estimates the effective density of flocs from an observed size-versus-settling-velocity relationship (Syvitski et al., 1995; Curran et al., 2002, 2004a;

Fox et al., 2004). Size-dependent effective densities are multiplied by floc volumes in a range of size classes to estimate the mass in suspension bound within flocs. That mass is divided by the total mass in suspension to obtain the floc fraction. Stokes' Law however applies to smooth, impermeable spheres under non-turbulent flow in which viscous forces dominate (Hawley, 1982). Such conditions are not typical for natural particles settling in marine environments. A second method uses the disaggregated inorganic grain size (DIGS) distribution of the seabed to estimate the relative proportion of suspended sediment deposited within single grains and flocs (Curran et al., 2004b; Fox et al., 2004). A third method estimates the bulk effective density of the suspension by dividing the total suspended solids concentration within a known volume of fluid by the total volume concentration of flocs observed within that fluid (Mikkelsen and Pejrup, 2001; Fox et al., 2004). The bulk effective density for the suspension and median floc diameter are used to estimate the bulk settling velocity of the suspension, which represents the settling velocity when the suspension is fully flocculated ($f = 1$). The bulk settling velocity is compared to the clearance rate of the suspension estimated from an observed size versus settling velocity relationship. The ratio of the clearance rate to bulk settling velocity is proportional to the fraction of flocs in suspension.

Studies that have estimated f indicate that the majority of fine sediment in suspension is flocculated (Syvitski et al., 1995; Curran et al., 2002, 2004a; Fox et al., 2004). Syvitski et al. (1995) observed that more than 90% of the suspended mass below the surface layer in Halifax Harbour, Canada, was bound within flocs greater than $50\ \mu\text{m}$ in diameter. Curran et al. (2002) observed floc fractions near 100% below the Eel River flood plume, northern California, for flocs greater than $125\ \mu\text{m}$ in diameter. Highly flocculated suspensions of flocs greater than $125\ \mu\text{m}$ in diameter were also observed below a glacial meltwater plume in Disenchantment Bay, Alaska, and below discharge plumes proximal to the Po River mouth, Italy (Curran et al., 2004a; Fox et al., 2004).

Methods for quantifying f provide insight into the fraction of mass in suspension bound within flocs, but do not describe the distribution of mass apportioned into component particles, microflocs, and macroflocs. A method to estimate the fraction of mass bound within different particle sizes would improve understanding of the behavior of fine

sediment in suspension and its affect on water column properties. This study estimates the fraction of mass in suspension bound within component particles, microflocs, and macroflocs, using the particle mass size distribution from $2\ \mu\text{m}$ to $1\ \text{cm}$ in diameter. Variations in the in situ size distributions of particle volume, particle projected area, particle mass, and particle settling mass flux in the bottom boundary layer offshore of the Têt River mouth, Gulf of Lions, France, were tracked through time.

2. Methods

2.1. Overview

The continental shelf in the Gulf of Lions, France, is narrow and crescent shaped with a heavily incised slope at the shelf break (water depth of $120\ \text{m}$), which descends to the adjacent Algero-Balearic Basin (Courp and Monaco, 1990). In the southern Gulf of Lions, strong Tramontane winds blow from the north-northwest between the Pyrenees and the Massif Central Mountains throughout the year and generally result in a southward flowing current associated with coastal downwelling (Estournel et al., 2003). Mean Tramontane wind speeds are $10\text{--}15\ \text{m s}^{-1}$, and the mean southward flowing current speed is $0.2\ \text{m s}^{-1}$. In rare instances Tramontane winds blow from the west-northwest and the coastal current flows northward. Strong winds blowing from the southeast, associated with lows passing over the basin, strongly influence sediment transport due to the generation of large wind waves and intense alongshore currents (Ferré et al., 2005). Tides are small on a regional scale and do not affect the circulation.

More than $10.5 \times 10^6\ \text{t}$ of sediment, mostly fine-grained, is discharged to the Gulf of Lions annually, with the Rhône River to the northeast being the source of up to 80% of the mass (Courp and Monaco, 1990). The shelf is characterized by low annual sediment inputs that vary between years, with the exception of the Rhône River submarine delta. In the southwest region of the Gulf of Lions, the Têt River mouth prodelta is characterized by a muddy bottom deposit that occupies the inner-shelf. The Têt River is flood dominated, and the sediment supply is limited by flow regulation.

In this study, the Têt River Buoy Site was the location of an in situ Size and Settling Column Tripod (INSSECT) deployment from April 18, 2005

at 1200 GMT to April 22, 2005, at 1200 GMT (Fig. 1). The Têt River Buoy Site is located in $28\ \text{m}$ water depth and is approximately $2.5\ \text{km}$ offshore of the Têt River mouth (LAT: 42°N 70.883 , LON: 3°E 06.647). The INSSECT is a multi-instrumented tripod designed to measure fine sediment properties close to the seabed in coastal environments (Mikkelsen et al., 2004). It was equipped with a digital floc camera (DFC), a digital video camera (DVC) and settling column, a LISST-100 Type B laser particle size analyzer, a compass/tilt sensor, and a sediment trap system that rotates under the DVC settling column.

The LISST-100 Type B laser particle size analyzer measures the volume concentration distribution of particles $1.25\text{--}250\ \mu\text{m}$ in diameter and the DFC the volume concentration distribution of particles $125\ \mu\text{m}\text{--}1\ \text{cm}$ in diameter. The DVC measures particles $226\ \mu\text{m}\text{--}5\ \text{mm}$ in diameter and is used to estimate the size versus settling velocity of particles in suspension. The compass/tilt sensor measures the orientation and tilt of the INSSECT. During the deployment, the DFC and LISST-100 were synchronized to take measurements every 15 min, while the DVC captured a 1 min video clip every 90 min. Compass/tilt was recorded every minute. The DFC was positioned $1.7\ \text{m}$ above the bottom (mab), and the LISST-100 and the top of the DVC settling column system were positioned $1.5\ \text{mab}$. The sediment trap system provides measure of the sediment flux that can later be analyzed for settling mass flux and the DIGS distribution.

Surface wave height and wave period, and current velocity, current direction, and water temperature at $2.5\ \text{mab}$, were measured using a bottom-mounted, upward-looking RDI 600 kHz ADCP deployed on a buoy less than $500\ \text{m}$ from the INSSECT. Estimates of combined wave-current bottom shear stress were made using the model of Grant and Madsen (1986). Salinity at $2.5\ \text{mab}$ was not measured throughout the deployment, although conductivity, temperature, and depth (CTD) profiles were collected opportunistically. Wind data was acquired from Météo France at Torreilles (the French National Weather Data Centre Station 66212001), approximately $9\ \text{km}$ northwest of the deployment site.

2.2. Particle size distributions

The raw LISST-100 data were inverted with manufacturer's software that outputs volume concentration distributions using a factory calibration

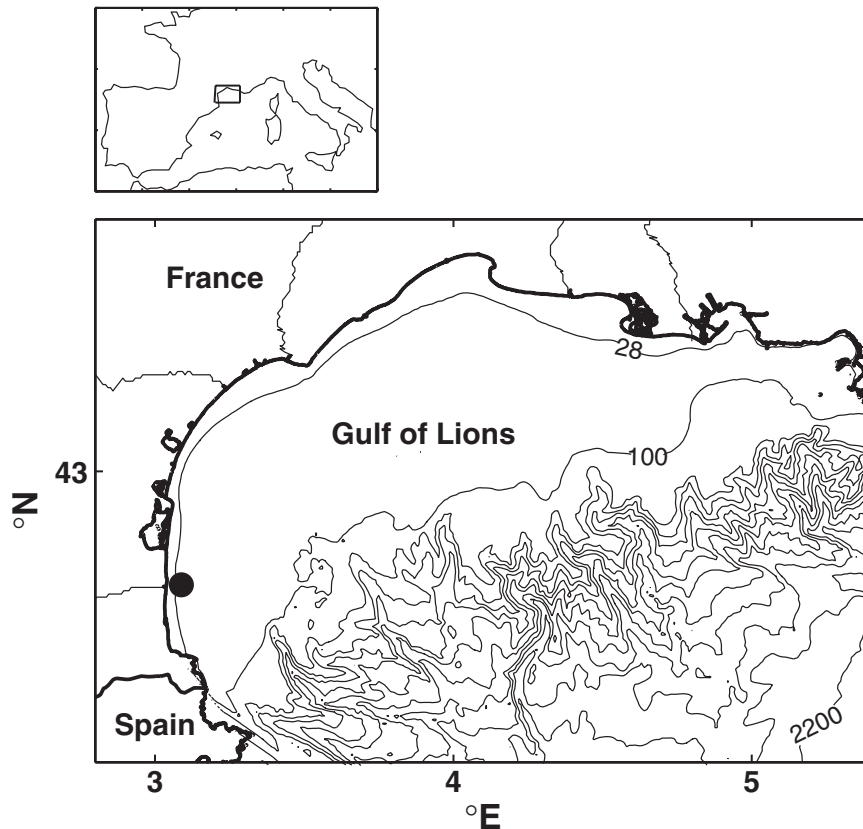


Fig. 1. Site map of the Gulf of Lions study area, France. The INSSECT deployment site was at 28 m water depth approximately 2.5 km offshore of the Têt River mouth, marked by the filled circle. Isobaths greater than 100 m increase at 200 m intervals from 200 to 2200 m. Wave height, wave period, current velocity, and water temperature were measured at an adjacent buoy less than 500 m from the INSSECT. Wind data was acquired from Météo France at Torreilles (Station 66212001), approximately 9 km northwest of the deployment site.

of the scattering pattern of particles of known size and volume concentration (Traykovski et al., 1999; Agrawal and Pottsmith, 2000; Mikkelsen et al., 2005). For each sample period, 6 volume concentration distributions were collected over 30 s. The mean volume concentration distribution was used to represent each sample time. The LISST-100 volume concentrations ($\text{mm}^3 \text{L}^{-1}$) were binned into size classes with logarithmically spaced diameter midpoints between 1.25 and 250 μm . The DFC images were analyzed using the same area of interest (AOI) for each image, and the threshold value (gray scale value that defines particle edges from the image background) for each image was user defined. Particle areas in the AOI of each image were converted to equivalent circular diameters. Particle volumes were estimated assuming spherical geometry. The volume concentrations ($\text{mm}^3 \text{L}^{-1}$) were binned into size classes with logarithmically spaced diameter midpoints between 125 μm and 1 cm.

Particles in suspension smaller than 1.25 μm in diameter result in an overestimate of volume by the LISST-100 in the smallest size classes, believed to be caused by scattering from such small, irregularly shaped particles (Agrawal, pers. comm.). Particles in suspension larger than 250 μm still scatter light and can also cause an overestimate of volume in the largest size classes (Agrawal and Pottsmith, 2000). In this study, there was an overestimate of volume by the LISST-100 in the smallest size classes so the smallest three bins were removed. In the largest three bins the LISST-100 under-estimated the volume concentration compared to the DFC by up to several orders of magnitude, so they were also removed. The result was LISST-100 volume concentration distributions ranging from 2 to 165 μm in diameter. After trimming the LISST-100 and DFC volume concentration distributions, only one size bin overlapped between the two instrument distributions. The LISST-100 volume concentrations

in each size bin were multiplied by the ratio of the DFC to LISST-100 volume concentrations in the overlapping size bin to reconcile the volume concentration difference between the two instruments. The mean adjustment factor (\pm standard deviation) for all merged distributions was 2 ± 0.8 , and was similar to that observed by Mikkelsen et al. (2005). The particle projected area concentration distributions were estimated from the merged particle volume concentration distributions assuming spherical geometry.

2.3. Particle settling velocity (w_f) and effective density ($\rho_f - \rho_w$)

The DVC settling column was equipped with a baffled top to minimize flow disruptions of settling particles within the column. Particle settling velocities estimated from the DVC were combined into a floc size versus settling velocity and floc size versus effective density relationship for the entire deployment, following the procedure of Fox et al. (2004). Floc effective densities were estimated from the observed floc settling velocities using Stokes' Law. These were fit to the model of Khelifa and Hill (2006) to estimate the effective density of particles $2 \mu\text{m} - 1 \text{ cm}$ in diameter. Observations suggest that flocculated suspensions exhibit a range of particle sizes that cannot be characterized by a single fractal dimension, as the packing arrangement of component particles within flocs changes as a function of size (Li and Logan, 1995; Dyer and Manning, 1999). The Khelifa and Hill (2006) model accounts for a decrease in floc density with an increase in floc size in a way that is consistent with observations from 26 published data sets. In the model, particle effective density follows the form

$$\rho_f - \rho_w = (\rho_s - \rho_w) \left(\frac{D}{d_c} \right)^{F-3}, \quad (1)$$

where ρ_f is the floc effective density, ρ_w is the density of seawater, ρ_s is the average density of the floc component grains, D is the particle diameter in a given size class, d_c is the median component grain diameter in flocs, and F relates particle mass to particle diameter. It is akin to a size-specific fractal dimension. For particle sizes less than or equal to the median component grain diameter the effective density is equal to the average density of the floc component grains. The settling velocities for parti-

cles $2 \mu\text{m} - 1 \text{ cm}$ in diameter were estimated with

$$w_s = \frac{1}{18} \theta g \frac{\rho_s - \rho_w}{\mu} d_c^{3-F} \frac{D^{F-1}}{1 + 0.15 \text{Re}^{0.687}}, \quad (2)$$

where w_s is the particle settling velocity, θ is the particle shape factor (assumed to be spheres, where $\theta = 1$), g is the gravitational acceleration, μ is the dynamic viscosity of seawater, and Re is the particle Reynolds number (Khelifa and Hill, 2006). Particle mass concentration distributions were estimated from the particle volume concentration distributions using the size-specific particle effective densities estimated from Eq. (1). Particle settling mass flux distributions were estimated from the particle mass concentration distributions using the size-specific particle settling velocities estimated from Eq. (2).

3. Results

The INSSECT was deployed at 1200 GMT on April 18, 2005. Throughout the deployment, winds predominantly blew from the northwest at $< 10 \text{ m s}^{-1}$. In the late morning of April 19, the wind shifted and blew from the southeast at $< 5 \text{ m s}^{-1}$ until early afternoon, when it strengthened and shifted back to the northwest (Fig. 2). On April 22, the winds decreased to $< 5 \text{ m s}^{-1}$ for the remainder of the deployment period. The bottom current predominantly flowed northward at $< 0.1 \text{ m s}^{-1}$ early in the deployment. It increased to 0.18 m s^{-1} at 0745 GMT on April 20, then decreased and flowed southward at approximately 0.1 m s^{-1} on April 22, following the decrease in wind speeds at midday on April 21 (Fig. 2). The significant wave height was generally $< 0.3 \text{ m}$ during the deployment, although significant wave heights $> 0.5 \text{ m}$ were observed on April 20 due to a localized weather event that resulted in wind blowing from the southeast on April 19 (Fig. 2). The peak wave period ranged from 2 to 9 s during the deployment, with the shortest wave periods associated with the peak wind wave event on April 20.

The combined wave-current bottom shear stress was generally $< 0.04 \text{ Pa}$, although fluctuations in bottom shear stress occurred throughout the deployment (Fig. 2). The highest bottom shear stress of 0.039 Pa during the deployment was observed on April 20 at 0745 GMT, when the current velocity and significant wave height were at a maximum



Fig. 2. Wind speed, current speed at 2.5 m above bottom (mab), significant wave height, combined wave-current bottom shear stress, and water temperature at 2.5 mab at the Têt River Buoy Site. INSSECT was deployed from April 18, 2005 at 1200 GMT to April 22, 2005, at 1200 GMT. Wind speed is indicated by stick length and wind direction is indicated by stick orientation. Positive wind speeds represent winds blowing from the south and negative wind speeds represent winds blowing from the north. Bottom current speed and current direction are similarly represented in the second panel. Positive bottom current speeds represent currents flowing from the south and negative bottom current speeds represent currents flowing from the north.

(Fig. 2). The elevated bottom shear stress was short-lived and returned to <0.02 Pa by 1045 GMT on April 20, where it remained for the remainder of the deployment period. The water temperature at 2.5 mab was relatively constant at 12.6°C during the first 72 h of the deployment (Fig. 2). On April 20, the water temperature increased to 12.7°C at 0315 GMT. The temperature slowly increased to a maximum of 12.8°C by the end of the day and then

again increased to 13°C at 1045 GMT on April 21. The temperature then decreased to 12.9°C prior to the INSSECT recovery on April 22.

Digital video of settling flocs resulted in 1044 independent estimates of in situ floc size and settling velocity at 1.5 mab. Observed settling velocities ranged from 0.2 to 32.3 mm s^{-1} for flocs $226.1\text{ }\mu\text{m}$ – 1.7 mm in diameter (Fig. 3). The data were binned into logarithmically-spaced diameter size classes. Median settling velocity as a function of diameter followed the expression:

$$w_f = 0.004d_f^{0.77} (r^2 = 0.96), \quad (3)$$

where w_f is the floc settling velocity (mm s^{-1}) and d_f is the binned floc equivalent spherical diameter (μm) (Fig. 3). Settling velocities estimated from Eq. (2) ranged from 0.3 to 1.2 mm s^{-1} for binned flocs sizes $263.1\text{ }\mu\text{m}$ – 1.6 mm in diameter (Fig. 3).

Floc effective densities estimated using Stokes' Law ranged from 465.7 to 1.1 kg m^{-3} for flocs $226.1\text{ }\mu\text{m}$ – 1.7 mm in diameter (Fig. 3). Median floc size versus effective density as a function of diameter followed the expression:

$$\rho_f - \rho_w = 7971d_f^{-1.19} (r^2 = 0.98), \quad (4)$$

where $\rho_f - \rho_w$ is the floc effective density (kg m^{-3}). Floc effective densities estimated from Eq. (4) ranged from 10.5 to 1.2 kg m^{-3} for binned flocs $263.1\text{ }\mu\text{m}$ – 1.6 mm in diameter (Fig. 3).

The density of seawater (ρ_w), estimated from a CTD profile taken at the time of the INSSECT deployment, was 1029 kg m^{-3} . The median component grain size diameter within flocs (d_c) and sediment density (ρ_s) were adjusted to fit the [Khelifa and Hill \(2006\)](#) model to the observed particle settling velocity and effective density data (Fig. 4). The values of d_c and ρ_s were $5\text{ }\mu\text{m}$ and 1600 kg m^{-3} , respectively. Settling velocities estimated from the [Khelifa and Hill \(2006\)](#) model ranged from 0.3 to 1.5 mm s^{-1} for particles $263.1\text{ }\mu\text{m}$ – 1.6 mm in diameter. Effective densities estimated from the [Khelifa and Hill \(2006\)](#) model ranged from 11.4 to 1.4 kg m^{-3} for particles $263.1\text{ }\mu\text{m}$ – 1.6 mm in diameter. At particle diameters $<\sim 5\text{ }\mu\text{m}$ the modeled effective densities were constant at 571 kg m^{-3} , which is the mean effective density for small component particles.

The particle volume concentration, particle projected area concentration, particle mass concentration, and particle settling mass flux distributions were apportioned into component particle ($<36\text{ }\mu\text{m}$

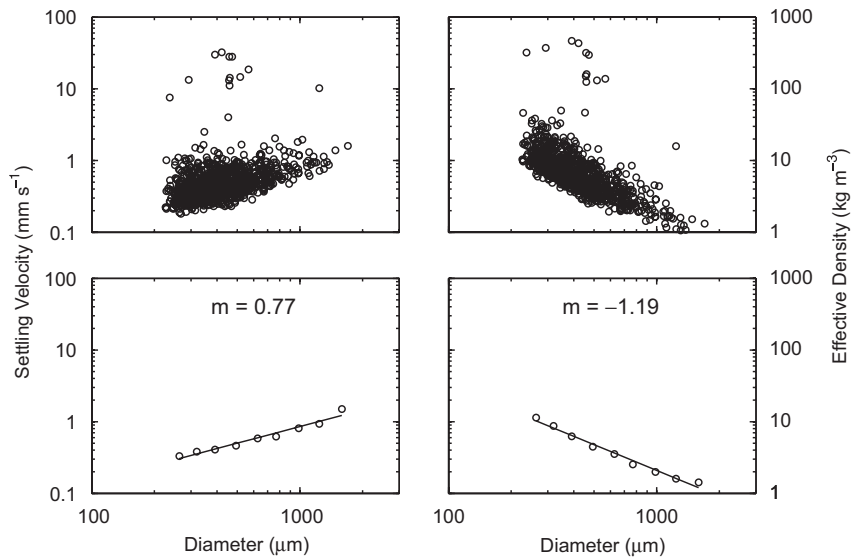


Fig. 3. Unbinned particle size versus settling velocity and particle size versus effective density during the deployment period (upper panels, $n = 1044$). The particle effective density was estimated by rearranging Stokes' Law. The lower panels exhibit the median particle size versus settling velocity and particle size versus effective density relationships for binned data, where 'm' is the slope.

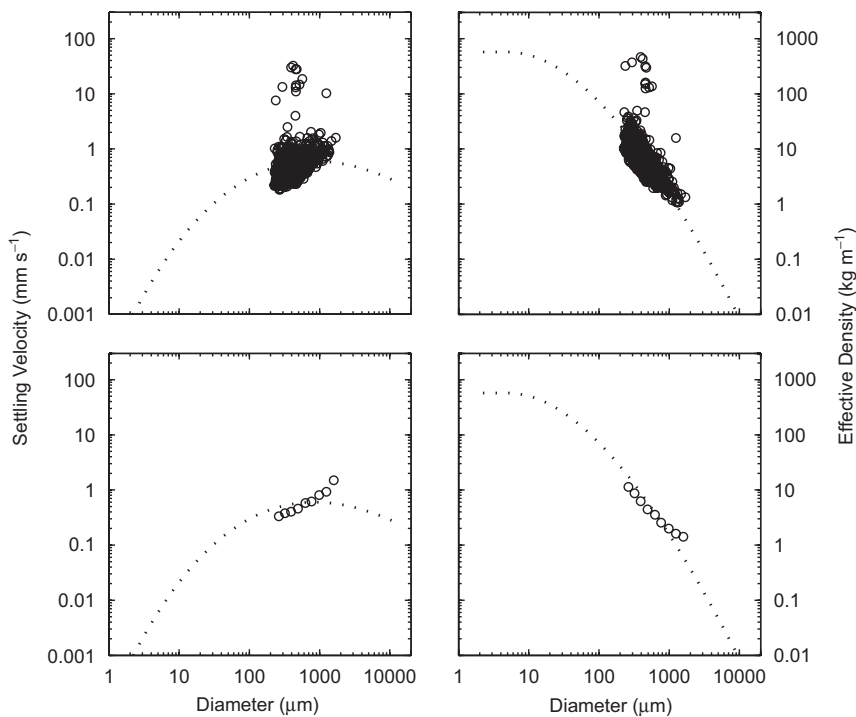


Fig. 4. Unbinned, observed particle size versus settling velocity and particle size versus effective density estimated using Stokes' Law during the deployment period (open circles, upper panels) versus estimates from the [Khelifa and Hill \(2006\)](#) model (dashed line, upper panels). Lower panels demonstrate the median of binned particle size versus settling velocity and particle size versus effective density data presented in the upper panels (open circles) versus estimates from the [Khelifa and Hill \(2006\)](#) model (dashed line).

in diameter), microfloc (36–133 μm in diameter), and macrofloc ($> 133 \mu\text{m}$ in diameter) fractions. These boundaries differ slightly from those of [Eisma](#)

(1986) due to the logarithmically spaced diameter midpoints of the merged particle size distributions used in this study. The suspension composition

based on particle volume concentration was dominated by the macrofloc fraction throughout the deployment. On average, 85.4% of the volume concentration in suspension was accounted for by macroflocs, 7.2% by microflocs, and 7.4% by component particles (Fig. 5). Throughout the deployment the percentage of component particles and microflocs by volume increased slightly. Following the suspension event on April 19, the absolute volume concentration remained relatively constant, while the component particle and microfloc percentages slightly increased (Fig. 5).

The increase in the component particle fraction in suspension throughout the deployment was more obvious when the suspension was represented by particle projected area concentration and particle mass concentration. Based on the projected area concentration of particles, the suspension composition was dominated by the component particle throughout the deployment. On average, 66.2% of the particle projected area concentration in suspension was accounted for by component particles, 7.8% by microflocs, and 26% by macroflocs (Fig. 5). The suspension composition based on particle mass concentration was also dominated by

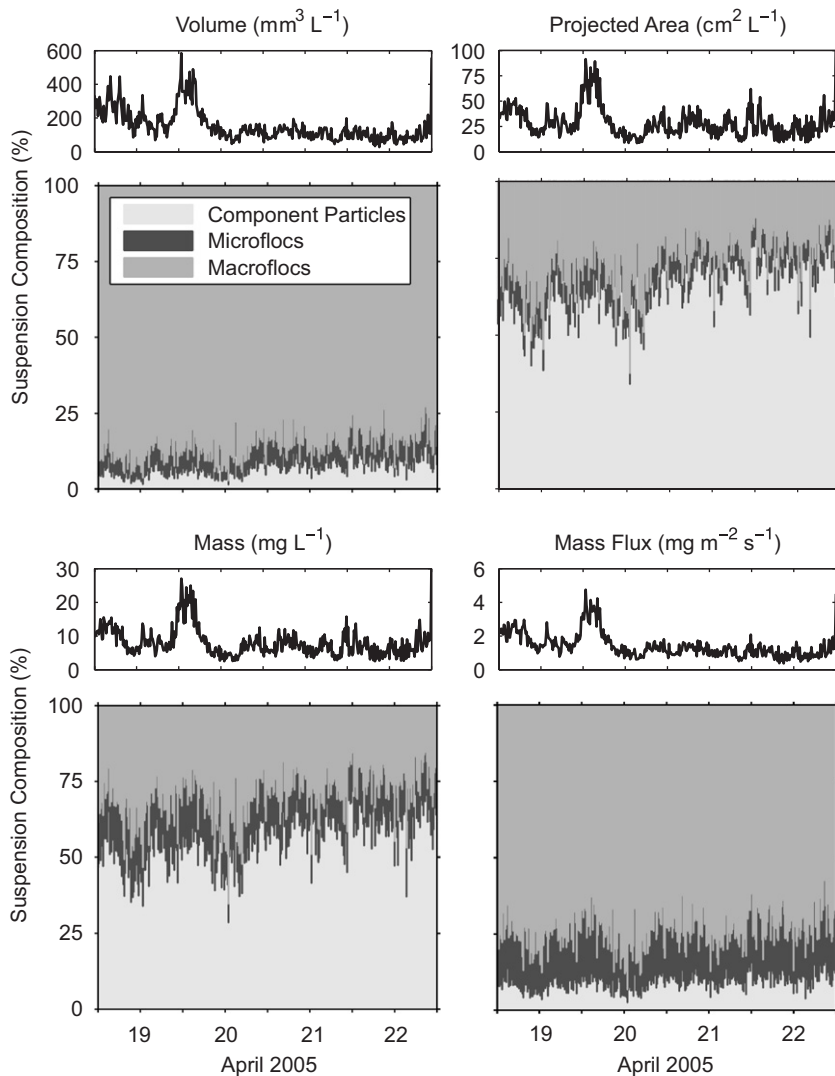


Fig. 5. Particle volume concentration, particle projected area concentration, particle mass concentration, and particle settling mass flux apportioned into component particle ($<36 \mu\text{m}$ in diameter), microfloc ($36\text{--}133 \mu\text{m}$ in diameter), and macrofloc ($>133 \mu\text{m}$ in diameter) fractions.

the component particle fraction. On average, 56.4% of the particle mass concentration in suspension was accounted for by component particles, 14.3% by microflocs, and 29.3% by macroflocs (Fig. 5). The highest macrofloc fractions by particle projected area and particle mass were observed following the suspension events in the afternoons of April 18 and 19 (Fig. 5).

The particle suspension composition based on the settling mass flux was dominated by the macrofloc fraction throughout the deployment. On average, 73.5% of the particle settling mass flux was accounted for by macroflocs, 17.1% by microflocs, and 9.4% by component particles (Fig. 5). Elevated periods of particle settling mass flux of macroflocs followed the resuspension events in the afternoons of April 18 and 19. The absence of a subsequent resuspension event during the elevated bottom shear stress period of April 20 suggests that sediments resuspended prior to April 20 were advected from the field site rather than re-deposited on the seabed.

4. Discussion

Increase in the suspended sediment concentration late in the morning of April 19 was likely associated with resuspension of a loosely consolidated mud layer deposited prior to the survey, which was resuspended by the bottom shear stress in excess of 0.01 Pa in the afternoon of April 18 and morning of April 19 (Fig. 2). Bottom shear stress in the range of 0.01–0.02 Pa has been observed to resuspend aggregate ‘fluff’ layers off the seabed (Thomsen and Gust, 2000; Schaaff et al., 2002, 2006; El Ganaoui et al., 2004). The resuspended sediment was likely advected from the field site by the strong northward bottom current observed at this time, and subsequent increases in bottom shear stress were not sufficient to resuspend the more consolidated underlying sediments that mobilize at shear stresses in excess of 0.04–<0.1 Pa (Thomsen and Gust, 2000; El Ganaoui et al., 2004; Schaaff et al., 2006). Following the resuspension event on April 19 there was a small increase in the component particle fraction in suspension throughout the remainder of the deployment period.

Increase in the component particle fraction in suspension was associated with an increase in water temperature. The increase in bottom water temperature may be considered a proxy for physical change in the bottom water mass. The cause of change in the bottom temperature may have been

advection or the downward mixing of surface water. It is believed that the increase in the component particle fraction was associated with a transient population of small particles that entered the field site within the warm water mass. Advection or downward mixing as the source of the small particles was supported by CTD profiles collected around the deployment site, which demonstrated an increase in bottom water temperature and conductivity between April 18 and 22, indicating the intrusion of warmer and saltier water during this period.

The observed size versus settling velocity and size versus effective density relationships were similar to those observed in other estuaries and fjords, and on continental shelves (Kranck et al., 1993; Fennessy et al., 1994; Hill et al., 1998; Dyer and Manning, 1999; Sternberg et al., 1999; Fox et al., 2004). Particles exhibited significant differences in settling velocity and effective density between particles sizes, and particles of similar size also exhibited differences in settling velocity and effective density by up to an order of magnitude (Fig. 3). The volume distributions 2 μm –1 cm in diameter and particle effective densities provided for the first time estimates of the particle mass concentration in suspension bound within component particles, microflocs, and macroflocs, as well as the settling mass flux to the seabed of these size fractions (Fig. 5).

Suspension composition by particle volume concentration and particle settling mass flux varied similarly through time, as did suspension composition by particle projected area concentration and particle mass concentration (Fig. 5). This is explained by similar scaling with diameter for particle volume and particle settling mass flux, and for particle projected area and particle mass. Particle volume scales with particle diameter cubed (d^3) and particle projected area scales with particle diameter squared (d^2). Particle mass is the product of particle volume and particle density and in this study scaled with particle diameter raised to the power 1.81. Particle settling mass flux is the product of particle mass and particle settling velocity and in this study scaled with particle diameter raised to the power 2.56. These relationships are dependent on the floc packing arrangement and are not necessarily true for all environments.

Previous methods that estimate the floc fraction (f) in suspension only characterize the abundance of large flocs, not the abundance of all particle sizes (Syvitski et al., 1995; Mikkelsen and Pejrup, 2001;

Curran et al., 2002, 2004a; Fox et al., 2004). Each method exhibits limitations. In the method that uses seabed size distributions, estimates of the fraction of mass deposited within flocs does not distinguish between the macrofloc and microfloc populations, and also assumes that all floc sizes can be characterized by a single floc settling velocity. This results in inaccurate estimates of f since flocs do not exhibit a single settling velocity. In the method that uses the bulk density approximation, it is assumed that flocs in suspension can be represented by a single floc diameter and that observed suspension clearance rates for all particle sizes can be estimated from an observed size versus settling velocity relationship. This results in inaccurate estimates of f since the settling velocities of small particles are not accurately estimated from an observed size versus settling velocity relationship, and again, flocs do not exhibit a single settling velocity.

The method for approximation of f that relies on Stokes' Law is a comparable approach to that presented in this study, as it makes use of an observed size versus settling velocity relationship to estimate particle effective density. Fox et al. (2004) argued that f was a factor of 2–3 times higher than it should be when estimated using the Stokes' approximation. In a study by Li and Logan (1997) it was observed that Stokes' Law underestimated the settling velocity of flocs by a factor of 2–3. The underestimate was attributed to reduced drag forces on sinking flocs caused by water passing through their porous and permeable interiors. If it is assumed that Stokes' Law underestimates the settling velocity of flocs by a factor of 2–3, then the estimate of floc density may be overestimated by this factor (Fox et al., 2004). The result is an overestimate of mass bound within individual flocs. In this study, floc effective densities were estimated from Stokes' Law and used to estimate particle effective densities with the Khelifa and Hill (2006) model. If particle effective densities estimated using Stokes' Law were overestimated by a factor of 2–3 the absolute mass within flocs presented in this study would also be overestimated by this factor (Fig. 5). The relative proportion of mass among different particle size classes, however, would remain the same, since the overestimate of particle mass would apply to all size classes uniformly. Only the absolute mass and absolute settling mass flux would be overestimated by a factor of 2–3.

The Khelifa and Hill (2006) model makes use of suspended sediment characteristics to estimate

particle effective density. Upon recovery of IN-SSECT the flux cup sediment samples were lost, preventing estimate of the density of the floc component grains and the median component grain size diameter that act as input variables to the Khelifa and Hill (2006) model. As a result, particle effective densities estimated from Stokes' Law were used to fit the Khelifa and Hill (2006) model. Subsequent studies should quantify the density of the floc component grains and the median component grain size diameter from bulk sediment samples. This would prevent potential error in the estimate of particle effective densities due to the use of Stokes' Law. Measurement of the suspended mass concentration in situ would also permit comparison with the total particle mass concentration estimated from the particle size distributions.

Few studies have tracked changes in the entire suspended particle size distribution through time (Bale and Morris, 1987; Gibbs et al., 1989; Eisma et al., 1990; Mikkelsen et al., 2006). This is difficult as it often requires use of multiple instruments that analyze different particle sizes in suspension. Bale and Morris (1987) used a Malvern Instruments particle sizer to estimate changes in the in situ volume concentration distribution of particles 1.9–188 μm in diameter, in the Tamar Estuary, England. Gibbs et al. (1989) used an in situ holographic microscopic system and a ship board inverted microscope to estimate changes in the in situ volume concentration distribution of particles <200 μm in diameter, in the Gironde Estuary, France. Eisma et al. (1990) used an in situ camera system to estimate changes in the in situ volume concentration distribution of particles 3.6–644 μm in diameter, in the Scheldt Estuary, Netherlands. The studies demonstrated that changes in the volume concentration within different particle size classes can only be used to constrain relative changes in the floc fraction by volume in suspension, since flocs are porous and changes in volume concentration due to floc formation and floc breakup are non-conservative.

Mikkelsen et al. (2006) used an in situ digital floc camera and LISST-100 Type C to estimate changes in the in situ volume concentration distribution of particles 2.5 μm –1 cm in diameter, proximal to rivers discharging into the western Adriatic Sea, Italy. Results of the study indicated that when stress in the water column increased there was a decrease in the volume concentration of macroflocs in suspension accompanied by an increase in the volume concen-

tration of microflocs in suspension, presumably due to floc breakup and microfloc resuspension. As the stress decreased the volume concentration of macroflocs again increased and then rapidly decreased under calm conditions, presumably as macroflocs settled out of suspension. Mikkelsen et al. (2006) were unable to determine the absolute relationship between floc size and stress based on changes in the volume concentration distribution alone, due to other factors that contribute to changes in the volume concentration distribution such as sediment deposition, resuspension, advection, and microbial mediation.

Caution must be taken when characterizing suspension composition by the particle volume distribution, because a few large particles in suspension can represent a significant fraction of the total volume (Droppo et al., 2005), but not necessarily a significant fraction of the total mass. In this study it was difficult to detect temporal increases in the percentage of component particles in suspension by changes in the particle volume concentration distribution. The increase was more easily detected by changes in the distribution of particle mass. Particle mass concentration better reveals the behavior of the component particle fraction because small particles have more mass per unit volume than large porous flocs, due to their higher densities.

The increase in the component particle mass fraction in suspension observed between April 20 and the end of the deployment affected the optical properties of the water column. The beam attenuation coefficient, C , represents the fraction of light absorbed and scattered by particles in suspension as the light traverses a meter-thick parcel of water. Changes in C typically are attributed to changes in the suspended sediment concentration. The increase in C observed towards the end of the study period however was associated with an increase in the percentage of component particles in suspension and not an increase in the absolute suspended mass concentration (Fig. 6). The suspended mass concentration was relatively constant while the area-to-mass ratio increased due to the greater relative abundance of component particles (Fig. 6). Similar results for optical backscatter were observed by Gibbs and Wolanski (1992) and Hatcher et al. (2001) who detected changes in the projected-area of suspended particles due to changes in the suspension composition and not due to an increase in suspended concentration. These observations serve

as a reminder that changes in suspension optical properties may reflect changes in the projected-area in suspension due to floc formation and floc breakup rather than absolute changes in the suspended mass concentration.

The mean bulk effective settling velocity estimated from the suspension composition by mass concentration was 0.18 mm s^{-1} . The suspension clearance rate (or bulk effective settling velocity) decreased throughout the deployment as the fraction of mass bound within component particles increased (Fig. 7). Suspension composition by mass concentration may provide an explanation of observed clearance rates of fine sediment suspensions. In a study by Curran et al. (2002) on fine sediment dynamics in the Eel River flood plume,

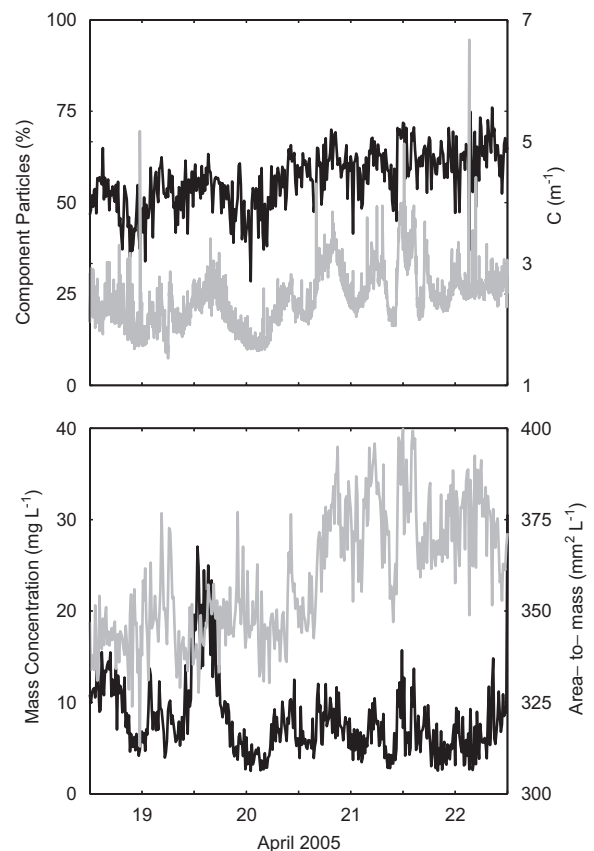


Fig. 6. Increase through time in the percentage of component particles in suspension by mass (black line, upper panel) has implications on water clarity as demonstrated by an increase in the beam attenuation coefficient, C , through time (gray line, upper panel). The mass concentration in suspension remains relatively constant from April 20 to the end of the deployment period (black line, lower panel), while the area-to-mass ratio in suspension increases due to the increased presence of component particles (gray line, lower panel).

it was observed that suspended sediments were primarily bound within large flocs that deposited on the order of 1 mm s^{-1} , although the estimated plume clearance rate was on the order of 0.1 mm s^{-1} . Curran et al. (2002) reconciled this difference by invoking advection of flocculated sediment from the nearshore that resupplied large flocs as they deposited in the offshore region of the plume. Similarly, in an unpublished study on dynamics in a glacial meltwater plume within an Alaskan fjord, plume clearance rates were estimated to be on the order of 0.1 mm s^{-1} despite the presence of a highly flocculated suspension and floc settling velocities on the order of 1 mm s^{-1} . Previous estimates of the floc fraction in suspension were often greater than 100% (Curran et al., 2002, 2004a; Fox et al., 2004), although this is not physically possible and likely arose from the overestimate of floc density due to Stokes' Law. Contradiction between predicted and observed bulk clearance rates of fine sediment suspensions thus may be explained by the overestimate of mass bound within large flocs due to the use of Stokes' Law to estimate f .

Due to the relatively quiescent environmental conditions observed during this study, results did not provide significant insight into the dynamics that control floc formation, breakup, deposition, and resuspension. This study did demonstrate that under calm conditions the majority of mass in suspension was bound within small component particles and not large flocs. As well, by observing

the particle mass distribution in suspension, small changes in the component particle fraction could be observed that were not easily detected by changes in the distribution of particle volume. This finding demonstrates that suspensions may be dynamic even in the absence of significant changes in forcing variables that control floc formation and breakup, and that a small change in suspension composition may affect water column properties (e.g. optical transmission). Last, estimates of the fraction of mass bound within component particles, microflocs, and macroflocs provide insight into the particle settling mass flux to the seabed, which may reconcile differences between predicted and observed bulk clearance rates of fine sediment suspensions.

5. Conclusion

In this study, measurements of floc size versus settling velocity and particle volume distributions $2 \mu\text{m}$ – 1 cm in diameter were made during relatively quiescent environmental conditions in a coastal bottom boundary layer. Particle effective density was estimated using Stokes' Law and the model of Khelifa and Hill (2006). The model relates particle mass to particle diameter with an exponent that varies as a function of particle size. The effective densities for all particle sizes were combined with the volume distributions to construct particle size distributions based on mass.

Results demonstrated that macroflocs only composed one quarter to one third of the suspension by mass throughout the deployment. The size versus settling velocity and size versus effective density observations were similar to those from other marine environments. Settling velocity scaled as diameter raised to a power just less than one, demonstrating that floc density decreased with increasing floc diameter. In addition, the binned settling velocities were tightly correlated with particle diameter, although variation in settling velocity within the size bins was large.

The abundance of component particles increased throughout the deployment. This was linked to an increase in water temperature and believed to be associated with advection or downward mixing of a different water mass at the field site. The total mass in suspension remained relatively constant between April 20 and the end of the deployment period. The increase in component particles reduced the optical transmission within the water column due to an increase in particle projected area per unit of mass.

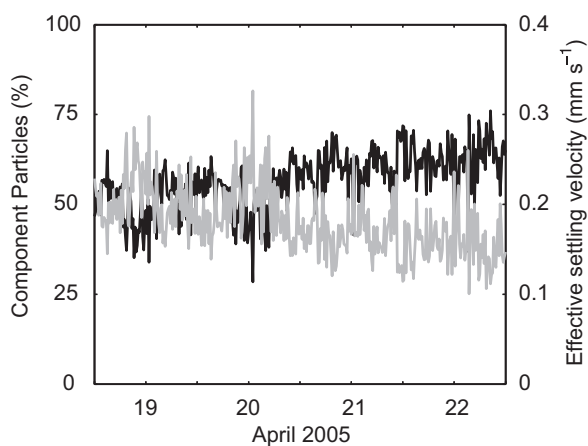


Fig. 7. Percentage of component particles in suspension by mass concentration (black line) and suspension bulk effective settling velocity (gray line). The bulk effective settling velocity decreases with an increase in the fraction of component particles in suspension. The mean bulk effective settling velocity for the deployment period was 0.18 mm s^{-1} .

Changes in the projected area of suspended particles due to floc formation and floc breakup, and not due to changes in the suspended mass concentration, underline the effect of fine sediment dynamics on water column properties (Gibbs and Wolanski, 1992; Hatcher et al., 2001).

The mean bulk effective settling velocity estimated from the mass distributions was 0.18 mm s^{-1} . This value was an order of magnitude lower than settling velocities observed for large flocs in suspension. Previous studies observed fine sediments to be bound within large flocs that settled out of suspension on the order of 1 mm s^{-1} , while estimated suspension clearance rates were of the order 0.1 mm s^{-1} (Curran et al., 2002). This study suggests that the difference between observed and predicted clearance rates may be explained by the overestimate of mass bound within flocs, due to the use of Stokes' Law to estimate particle effective density. The results of this study suggest that fine sediment suspensions may not be as highly flocculated as previously believed. Future studies should pursue similar observations within more energetic environments and at higher suspended sediment concentrations.

Acknowledgments

Sincere appreciation is given to the captain and crew of R/V *Endeavor* for their assistance in deploying field equipment. Thanks also to Jerome Bonnin for his logistical support in France in preparing for this cruise. This research was supported by the US Office of Naval Research (ONR), as part of the EuroSTRATAFORM program (contract N00014-04-1-0165 awarded to P.S. Hill and contract N00014-04-1-0182 awarded to T.G. Milligan).

References

- Agrawal, Y.C., Pottsmith, H.C., 2000. Instruments for particle size and settling velocity observations in sediment transport. *Marine Geology* 168, 89–114.
- Bale, A.J., Morris, A.W., 1987. In situ measurements of particle size in estuarine waters. *Estuarine, Coastal and Shelf Science* 24, 253–263.
- Courp, T., Monaco, A., 1990. Sediment dispersal and accumulation on the continental margin of the Gulf of Lions: sedimentary budget. *Continental Shelf Research* 10, 1063–1087.
- Curran, K.J., Hill, P.S., Milligan, T.G., 2002. Fine-grained suspended sediment dynamics in the Eel River flood plume. *Continental Shelf Research* 22, 2537–2550.
- Curran, K.J., Hill, P.S., Milligan, T.G., Cowan, E.A., Syvitski, J.P.M., Konings, S.M., 2004a. Fine-grained sediment flocculation below the Hubbard Glacier meltwater plume, Disenchantment Bay, Alaska. *Marine Geology* 203, 83–94.
- Curran, K.J., Hill, P.S., Schell, T.M., Milligan, T.G., Piper, D.J.W., 2004b. Inferring the mass fraction of floc-deposited mud: application to fine-grained turbidites. *Sedimentology* 51, 927–944.
- Droppo, I.G., Leppard, G.G., Liss, S.N., Milligan, T.G., 2005. Opportunities, needs, and strategic direction for research on flocculation in natural and engineered systems. In: Droppo, I.G., Leppard, G.G., Liss, S.N., Milligan, T.G. (Eds.), *Flocculation in Natural and Engineered Environmental Systems*. CRC Press, New York, pp. 407–421.
- Dyer, K.R., Manning, A.J., 1999. Observation of the size, settling velocity, and effective density of flocs, and their fractal dimension. *Journal of Sea Research* 41, 87–95.
- Dyer, K.R., Cornelisse, J., Dearnaley, M.P., Fennessy, M.J., Jones, S.E., Kappenberg, J., McCave, I.N., Pejrup, M., Puls, W., van Leussen, W., Wolfstein, K., 1996. A comparison of in situ techniques for estuarine floc settling velocity measurements. *Journal of Sea Research* 36, 15–29.
- Eisma, D., 1986. Flocculation and de-flocculation of suspended matter in estuaries. *Netherlands Journal of Sea Research* 20, 183–199.
- Eisma, D., Schuhmacher, T., Boekel, H., van Heerwaarden, J., Franken, H., Laan, M., Vaars, A., Eijjenraam, F., Kalf, J., 1990. A camera and image-analysis system for in situ observation of flocs in natural waters. *Netherlands Journal of Sea Research* 27, 43–56.
- El Ganaoui, O., Schaaff, E., Boyer, P., Amielh, M., Anselmet, F., Grenz, C., 2004. The deposition and erosion of cohesive sediments determined by a multi-class model. *Estuarine, Coastal and Shelf Science* 60, 457–475.
- Estournel, C., Durrieu de Madron, X., Marsaleix, P., Auclair, F., Julliand, C., Vehil, R., 2003. Observation and modeling of the winter coastal oceanic circulation in the Gulf of Lion under wind conditions influenced by the continental orography (FETCH experiment). *Journal of Geophysical Research* 108, 8059, doi:10.1029/2001JCO00825.
- Fennessy, M.J., Dyer, K.R., Huntley, D.A., 1994. INSSEV: an instrument to measure the size and settling velocity of flocs in situ. *Marine Geology* 117, 107–117.
- Ferré, B., Guizien, K., Durrieu de Madron, X., Palanques, A., Guillén, J., Grémare, A., 2005. Fine-grained sediment dynamics during a storm event in the inner-shelf of the Gulf of Lion (NW Mediterranean). *Continental Shelf Research* 25, 2410–2427.
- Fox, J.M., Hill, P.S., Milligan, T.G., Ogston, A.S., Boldrin, A., 2004. Floc fraction in the waters of the Po River prodelta. *Continental Shelf Research* 24, 1699–1715.
- Gibbs, R.J., Wolanski, E., 1992. The effect of flocs on optical backscattering measurements of suspended material concentration. *Marine Geology* 107, 289–291.
- Gibbs, R.J., Tshudy, D.M., Konwar, L., Martin, J.M., 1989. Coagulation and transport of sediments in the Gironde Estuary. *Sedimentology* 36, 987–999.
- Grant, W.D., Madsen, O.S., 1986. The continental shelf bottom boundary layer. *Annual Review of Fluid Mechanics* 18, 265–305.

- Hatcher, A., Hill, P.S., Grant, J., 2001. Optical backscatter of marine flocs. *Journal of Sea Research* 46, 1–12.
- Hawley, N., 1982. Settling velocity distribution of natural aggregates. *Journal of Geophysical Research* 87, 9489–9498.
- Hill, P.S., Syvitski, J.P.M., Cowan, E.A., Powell, R.D., 1998. In situ observations of floc settling velocities in Glacier Bay, Alaska. *Marine Geology* 145, 85–94.
- Khelifa, A., Hill, P.S., 2006. Models for effective density and settling velocity of flocs. *Journal of Hydraulic Research* 44, 390–401.
- Kranck, K., Petticrew, E., Milligan, T.G., Droppo, I., 1993. In situ particle size distributions resulting from flocculation of suspended sediment. In: Mehta, A.J. (Ed.), *Nearshore and Cohesive Sediment Transport*. Coastal and Estuarine Studies, vol. 42. Springer, New York, pp. 60–75.
- Li, X., Logan, B.E., 1995. Size distributions and fractal properties of particles during a simulated phytoplankton bloom in a mesocosm. *Deep Research II* 42, 125–138.
- Li, X., Logan, B.E., 1997. Collision frequencies of fractal aggregates with small particles by differential settling. *Environmental Science and Technology* 31, 1229–1236.
- Mikkelsen, O.A., Pejrup, M., 2001. The use of a LISST-100 laser particle sizer for in-situ estimates of floc size, density and settling velocity. *Geo-Marine Letters* 20, 187–195.
- Mikkelsen, O.A., Hill, P.S., Milligan, T.G., Moffatt, D., 2004. INSSECT—an instrumented platform for investigating floc properties close to the seabed. *Limnology and Oceanography: Methods* 2, 226–236.
- Mikkelsen, O.A., Hill, P.S., Milligan, T.G., Chant, R.J., 2005. In situ particle size distributions and volume concentrations from a LISST-100 laser particle sizer and a digital floc camera. *Continental Shelf Research* 25, 1959–1978.
- Mikkelsen, O.A., Hill, P.S., Milligan, T.G., 2006. Single-grain, microfloc and macrofloc volume variations observed with a LISST-100 and digital floc camera. *Journal of Sea Research* 55, 87–102.
- Schaaff, E., Grenz, C., Pinazo, C., 2002. Erosion of particulate inorganic and organic matter in the Gulf of Lion. *Comptes Rendus Geoscience* 334, 1071–1077.
- Schaaff, E., Grenz, C., Pinazo, C., Lansard, B., 2006. Field and laboratory measurements of sediment erodibility. *Journal of Sea Research* 55, 30–42.
- Sternberg, R.W., Berhane, I., Ogston, A.S., 1999. Measurement of the size and settling velocity of suspended aggregates on the northern California continental shelf. *Marine Geology* 154, 227–242.
- Syvitski, J.P.M., Asprey, K.W., Le Blanc, K.W.G., 1995. In situ characteristics of particles settling within a deep-water estuary. *Deep Sea Research II* 42, 223–256.
- Thomsen, L., Gust, G., 2000. Sediment erosion thresholds and characteristics of resuspended aggregates on the western European continental margin. *Deep-Sea Research I* 47, 1881–1897.
- Traykovski, P., Latter, R.J., Irish, J.D., 1999. A laboratory evaluation of the laser in situ scattering and transmissometry instrument using natural sediment. *Marine Geology* 159, 355–367.
- Xia, X.M., Li, Y., Yang, H., Wu, C.Y., Sing, T.H., Pong, H.K., 2004. Observations on the size and settling velocity distributions of suspended sediments in the Pearl River Estuary, China. *Continental Shelf Research* 24, 1809–1826.